Sleep and Breathing (2019) 23:103–115
https://doi.org/10.1007/s11325-018-1667-x

SLEEP BREATHING PHYSIOLOGY AND DISORDERS • ORIGINAL ARTICLE

Relationships among retropalatal airway, pharyngeal length, and craniofacial structures determined by magnetic resonance imaging in patients with obstructive sleep apnea

Suat Avci[1] · Hatice Lakadamyali[2] · Huseyin Lakadamyali[3] · Erdinc Aydin[1] · Mustafa Agah Tekindal[4]

Received: 31 May 2017 / Revised: 18 April 2018 / Accepted: 20 April 2018 / Published online: 5 May 2018

Abstract

Background The integration of anatomical and nonanatomical parameters will improve our ability to predict the outcomes of OSA treatment. Currently, no standardized, quantitative classification of upper airway anatomical traits is available. The retropalatal (RP) airway is the most important area to consider when planning anatomical treatment. However, current evaluation methods feature qualitative conventional endoscopy. Here, we describe a quantitative magnetic resonance imaging (MRI) method used to classify RP airway patterns.

Methods We recruited 117 males; 20 simple snorers and 97 patients with OSA. Lateral/anteroposterior ratios were calculated in three parallel planes and RP patterns were classified accordingly. Lateral wall soft tissue structures, skeletal dimensions representing those planes, pharyngeal lengths, and skeletal and vertical axis ratios were also measured.

Results Both the cross-sectional area at the hard palate level and the RP lateral dimension were associated with OSA. OSA patients had longer pharynges than controls. The oblique pattern was associated with narrow lateral dimensions. The vertical pattern was associated with a narrow nasopharynx but a longer pharynx. The airway ratio at the hard palate level and the skeletal ratios of all three planes were negatively correlated with the vertical axis ratio and together explained 40.8% of the variance in the vertical axis ratio.

Conclusions The data suggest that anatomical imbalances between the craniofacial skeletal and soft tissue structures affect pharyngeal airway morphology in all three dimensions. The dimensions of the nasopharynx, the cross-sectional area at the hard palate level, and pharyngeal length were associated not only with the RP patterns but also with OSA severity. This study affords insights into upper airway anatomy and RP patterns and may help diagnose OSA patients and aid in the selection of an appropriate therapy.

Keywords Sleep apnea · Airway · Quantitative retropalatal classification · Three-dimensional magnetic resonance imaging · Craniofacial structures

Presented at the 38th Turkish National Congress of Otorhinolaryngology and Head & Neck Surgery, Antalya, Turkey, October 27, 2016.

✉ Suat Avci
suat_avci2002@yahoo.com

[1] Department of Otolaryngology-Head and Neck Surgery, Baskent University, Ankara, Turkey

[2] Department of Radiology, Baskent University, Ankara, Turkey

[3] Department of Chest Disease, Baskent University, Ankara, Turkey

[4] Department of Biostatistics, Faculty of Veterinary Medicine, Selcuk University, Konya, Turkey

Introduction

Obstructive sleep apnea (OSA) is characterized by the recurrent partial or complete collapse of the upper airway during sleep. This causes intermittent hypoxemia, hypercapnia, and frequent cortical arousals [1]. Multiple features or "phenotypic traits" contribute to the pathogenesis of OSA. These include anatomical traits (a narrow/crowded/collapsible upper airway) and nonanatomical traits (waking up too easily during airway narrowing [a low respiratory arousal threshold], ineffective or reduced pharyngeal dilator muscle activity during sleep, and unstable ventilatory control [high loop gain]) [2, 3].

Although OSA is thus a heterogeneous disorder, a prerequisite for OSA development is a certain level of anatomical compromise/increased upper airway collapsibility [4]. Compared to those who do not have OSA, those with OSA generally have a smaller-diameter, longer, oval upper airway [5]. OSA treatment has traditionally targeted anatomical traits, and includes continuous positive airway pressure (CPAP), the placement of oral appliances, upper airway surgery, weight loss, and positional therapy. Such therapies are either often poorly tolerated (e.g., CPAP), difficult to perform (e.g., weight loss), or of variable and unpredictable efficacy (e.g., oral appliances) [4]. Both the diagnostic and treatment steps can be time-consuming, costly, and frustrating, especially for the many patients who fail CPAP [6].

Although most patients with moderate-to-severe OSA exhibit multilevel collapse, the soft palate is the most collapsible region of the upper airway [7]. In general, a change in the retropalatal (RP) shape from circular to elliptical, specifically laterally elliptical, is believed to be how CPAP [8] and oral appliances function [9]. Patients vary in their RP area responses to oral appliances and RP stimulation. Responders and nonresponders exhibit similar extents of retrolingual opening after stimulation, but responders develop greater increases in their RP areas [9]. One explanation is that the connections between the RP and retrolingual regions may vary among individuals [10].

From a surgical point of view, the baseline anatomical characteristics of patients have direct effects on how surgery changes the airway [11–14]. Patients with proximal RP airway narrowing (at 10 mm from the hard palate) do worse with classic uvulopalatopharyngoplasty (UPPP) than those with isolated distal narrowing (20 mm from the hard palate) [15]. Following surgery, responders demonstrate an increase in RP airway size, whereas nonresponders do not [12–14]. Selecting an appropriate surgical procedure is critical, but few guidelines are available [12]. Often the chosen technique reflects the surgeon's preference based on empirical experience, training, and ability. Thus, it is important to identify metrics other than those of polysomnography to guide upper airway surgery choices [12].

A recent review found that isolated cephalometric parameters could not be used to reliably predict treatment outcomes when mandibular advancement devices were placed, or surgery performed, to treat OSA [16]. Also, a recent systematic review of three-dimensional UAW anatomy suggested that no consensus had been attained on which anatomical variables of the upper airway were most relevant in terms of OSA pathogenesis, apart from a small minimum cross-sectional area [5].

Retropalatal patterns have been subdivided into oblique, vertical, and intermediate subtypes in an effort to better understand upper airway phenotypes and aid in surgical planning by Woodson [17]. Four landmarks are used: the hard palate, the genu, the velum, and the lateral pharyngeal walls [12, 18]. This classification suggests that upper pharyngeal narrowing occurs at the following locations: the velum (oblique pattern); the velum and genu (intermediate pattern); and the velum, genu, and hard palate (vertical pattern). The patterns are determined qualitatively during supine drug-induced sedation endoscopy (DISE) [17].

Traditional UPPP techniques focus on the velar segment of the soft palate and fail to address significant abnormalities in muscular and aponeurotic segments [12]. Palatal advancement addresses abnormalities of the aponeurotic and muscular segments and should be preferred in patients with proximal RP segment narrowing (from the hard palate level to 10 mm inferior to the hard palate). However, for an expansion sphincter pharyngoplasty procedure, patients should have an oblique pattern, and the narrowing should be close to the level of the velopharynx (~ 10–15 mm) [15, 19]. These data suggest that the upper part of the RP airway (from the hard palate to 20 mm inferior to the hard palate) is the most important segment informing the decision-making process for surgery for OSA [11–15, 17–19].

Thus, we focused on this region in this study. Previously, it was hypothesized that airway dimensions and pharyngeal length are functions of correlations between craniofacial soft and hard tissue structures [14]. However, to the best of our knowledge, no reported study has described quantitative measures for classifying RP patterns.

We aimed to develop a magnetic resonance (MR) imaging (MRI) method of classifying RP patterns quantitatively to determine whether significant differences in terms of parameter distributions are evident among OSA categories and RP pattern groups. We also sought to analyze correlations between RP patterns, pharyngeal length, and craniofacial soft and hard tissue structures and to confirm the utility of Woodson's model featuring three RP airway patterns.

Methods

Subjects

All 117 MR images were obtained between November 2015 and January 2018. Twenty simple snorers (apnea-hypopnea index [AHI] < 5 events/h) and 97 patients with OSA were evaluated. All patients were male, and all gave written informed consent. The study was approved by the Baskent University Institutional Review Board.

All patients had a clinical history taken and underwent physical and otolaryngology assessments, including (1) determination of body mass index (BMI), (2) conventional supine fiber-optic endoscopy via video recording when awake during routine clinical examination, (3) polysomnography, and (4) upper airway MRI. Exclusionary criteria included (1) age less than 18 years or more than 69 years; (2) taking of chronic medications that affect upper airway tone (e.g.,

benzodiazepines, sedatives); (3) tonsils of grades 3 or 4 or predominant central sleep apnea on polysomnography; (4) exclusions related to the use of MRI: (a) body weight > 125 kg (the table limit of the magnetic resonance scanner), (b) the presence of metallic implants (such as a pacemaker or ferromagnetic clips), or (c) severe claustrophobia; (5) severe chronic kidney, heart, or liver failure or abnormal lung function; and (6) other sleep disorders.

Subjects were divided into the following five categories based on the AHI: (1) normal/simple snoring: AHI < 5, (2) AHI 5 to < 15, (3) AHI 15 to < 30, (4) AHI 30 to < 50, and (5) AHI ≥ 50. In addition, all participants were subdivided into those with oblique, vertical, or intermediate patterns on MRI.

Polysomnography

All participants underwent polysomnography at the Baskent University Alanya Hospital Chest Disease Sleep Laboratory using a computerized polysomnography device (E series, 44 channels; Compumedics, Victoria, Australia). Sleep staging was performed according to American Academy of Sleep Medicine criteria [20, 21].

Magnetic resonance imaging

Magnetic resonance imaging (MRI) was performed on patients with OSA and simple snorers using a Brivo MRI 355 1.5 T (GE, Fairfield, CT, USA) with a quadrature head coil. Axial plane sections were obtained by T1-weighed MRI using fast spoiled gradient-echo (SPGR) 3D (TR/TE/FA, 6.2/1.8/12 ms; FOV, 254 × 254 mm; matrix, 186 × 186; NEX, 2). Slices (1.2 mm thick) were obtained from the nasion to the epiglottic vallecula (i.e., the base of the epiglottis). During axial MRI, all subjects were in the supine position with their heads placed in a neutral position to ensure consistent positioning. Each subject was examined during waking and tidal breathing for 7 min and 26 s. Fast SPGR 3D was chosen as the photography condition for MRI because this method can produce thin imaging sections and has high spatial resolution, a high signal-to-noise ratio, and the capability to reconstruct a desired plane.

Anatomical definitions, measurements, and analysis

A radiology specialist (HL) and an ENT specialist (SA) both measured the dimensions of the airways and craniofacial structures after selection of the images. SA performed all measurements at least three times on separate occasions to ensure reproducibility. If discrepancies were evident, or if the images were unclear, SA consulted the radiology specialist (HL).

A workstation with image-processing software (AW Volume Share 5; GE) was used to measure the MRI data; all linear measurements were expressed in millimeters.

Before performing measurements, we designated three planes. The A plane corresponded to the hard palate, and the B and C planes were parallel planes 10 and 20 mm inferior to the A plane, respectively (Fig. 1). Measurements were made on cross-sections of each plane to allow for quantitative classification of RP patterns (Fig. 1c–e). Our video archive of supine, awake, routine fiber-optic endoscopy procedures was used to determine RP airway ratio thresholds. Ten patients with apparently vertical RP airways were identified by reference to their cross-sectional airway MRI measurements. The lowest airway ratios were 1.45 for the A plane (R_1) and 1.50 for both the B and C planes (R_2 and R_3 respectively). Accordingly, airway ratio thresholds of 1.45 for the A plane and 1.50 for the B and C planes were used for quantitative classification of the remaining patients (Table 1).

The analyzed anatomical measures were separated into four independent domains (Table 2) :

(1) Cross-sectional airway parameters (Fig. 1c–e)

The airway dimensions of the A, B, and C planes were evaluated using multiple parameters, including three lateral and three anteroposterior dimensions, three latd/apd ratios describing the cross-sectional shapes of the airway, and the three cross-sectional areas (CSAs).

(2) Midsagittal parameters (Fig. 2)

Twelve landmarks were labeled in the midsagittal illustration, as were two lines and the mandibular plane. The sagittal anatomy was evaluated using seven linear parameters, three angular parameters, and one ratio.

(3) Cross-sectional soft tissue parameters (Fig. 3a)

Soft tissue structures surrounding the airway were evaluated using two linear parameters: pharyngeal fat pad thickness and pharyngeal wall thickness (the arithmetic means of bilateral measurements at the B and C planes).

(4) Cross-sectional skeletal parameters (Fig. 3a–c)

Skeletal structures surrounding the airway were evaluated using four linear and three ratio parameters.

Statistical analysis

For both discrete and continuous variables, descriptive statistics (means, standard deviations, frequencies, and percentiles) are given. The homogeneity of variance was checked using Levene's test. Normality was tested with the aid of the

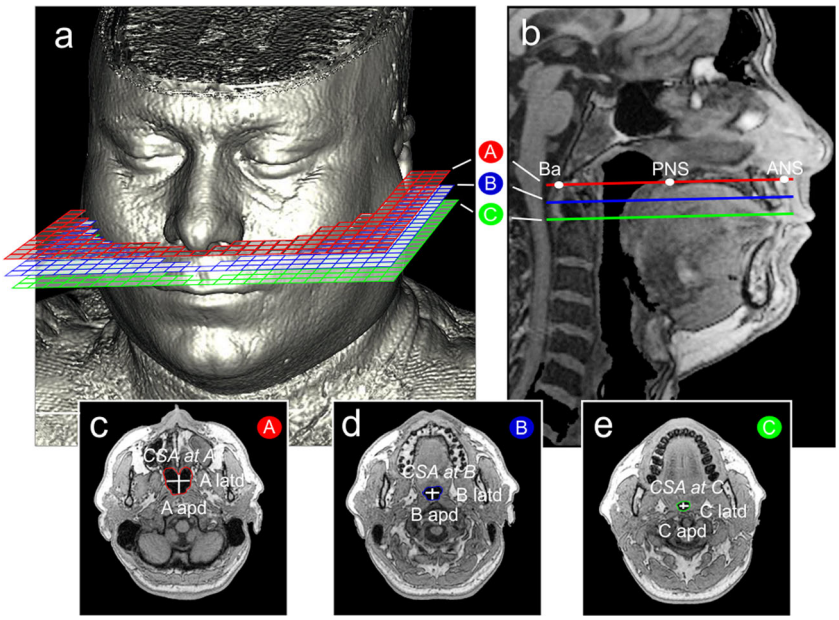

Fig. 1 **a** A representative three-dimensional MR image demonstrating the A, B, and C planes. **b** The A, B, and C planes on mid-sagittal MRI. Ba, basion; PNS, posterior nasal spine; ANS, anterior nasal spine. Cross-sections: **c** A plane, **d** B plane (a plane 10 mm inferior to the A plane and parallel to the A plane), **e** C plane (a plane 20 mm inferior to the A plane and parallel to the A plane). Airway dimensions: apd, anteroposterior dimension; latd, lateral dimension. Airway area: CSA, cross-sectional area

Shapiro-Wilk test. To compare differences between the two groups, Student's *t* test was used when the parametric test prerequisites were fulfilled and the Mann-Whitney *U* test otherwise. To compare differences among three or more groups, one-way analysis of variance was used when the parametric test prerequisites were fulfilled and the Kruskal–Wallis test otherwise. The Bonferroni correction, a test of multiple comparisons test, was employed to evaluate the significance of comparisons among three or more groups using the chi-square test. The chi-square test was also used to explore the relationships between pairs of discrete variables. When the expected sources were < 20%, Monte Carlo simulation was performed to include such sources in analysis. Age and BMI served as covariates (to exclude their effects) in group comparisons. Relationships between pairs of continuous variables were assessed by calculating Pearson correlation coefficients when parametric test prerequisites were fulfilled and Spearman correlation coefficients otherwise. Partial correlations were calculated to adjust for the effects of BMI, age, and AHI. Multiple linear regression analyses were performed to show the effects of independent variables on continuous dependent variables. All statistical analyses were performed using SPPS ver. 20 (released in 2011; IBM, Armonk, NY, USA); p values < 0.05 and < 0.01 were considered significant.

Results

Table 3 presents data comparing patient characteristics and parameters among the five OSA categories. The controls (AHI < 5) were younger and lighter than OSA patients ($p < 0.01$). Airway lateral dimensions and the CSA at the A plane were significantly higher in controls than in OSA patients (both ps < 0.01). Pharyngeal length was longer in the AHI ≥ 50 category than in the others ($p < 0.01$). The mandibular plane hyoid distance (L_7) was significantly longer in the AHI ≥ 50 category than in the others ($p < 0.001$). The R_7 ratio was significantly lower in the AHI 30 to < 50 and AHI ≥ 50 categories than in the others ($p = 0.02$).

Table 4 compares patient characteristics and parameters among those with the three RP patterns. The airway lateral dimensions were shorter in those with the oblique pattern than those in the others ($p < 0.001$). The mean CSA in the A plane was less in those with the oblique pattern than those in the others ($p < 0.01$). The midsagittal L_1 was significantly shorter, and the L_4 significantly longer, in those with the vertical pattern than those in the others ($p < 0.001$).

Table 5 shows the distribution of RP patterns by OSA category.

Table 6 presents simple and partial correlations between the airway ratios (R_1, R_2, R_3) and skeletal ratios (R_4, R_5, R_6). Table 7 lists simple and partial correlations between the cross-sectional and vertical axis ratios (R_7). Table 8 lists the changes in the corrected R_7 values per unit of R_1, R_4, R_5, and R_6.

Discussion

Three of our findings may contribute to an understanding of the relationships between RP airway patterns, craniofacial structures, and OSA. First, narrow lateral nasopharyngeal dimensions, a small CSA at A, a relatively long pharynx, and a high tendency to develop OSA were characteristic of the oblique pattern. Second, narrow nasopharyngeal AP dimensions, a markedly increased pharyngeal length, and a moderate tendency to develop OSA were characteristic of the

Table 1 Ratio thresholds for the classification of retropalatal patterns

	Oblique	Vertical	Intermediate
R_1	< 1.45	> 1.45	< 1.45
R_2	< 1.50	> 1.50	> 1.50
R_3	< 1.50	> 1.50	> 1.50

Abbreviations as in Table 2

vertical pattern. Third, large nasopharyngeal dimensions, a large CSA at A, increased velar angulation, and a short pharynx (the intermediate pattern) were associated with a low tendency to develop OSA.

Potential bias and limitations of the study

Several potential limitations of the study should be discussed. Woodson reported that approximately half of patients (52%) were oblique, whereas 25% were vertical and 23% were intermediate [6, 17]. According to our MRI method, 43% of our patients were oblique, whereas 20% were vertical and 37% were intermediate (Table 4). The notable difference in the percentage of patients with the intermediate pattern may be attributable to the following differences in classification methods.

First, Woodson's classification was dynamic in nature, based on DISE and fiber-optic examinations performed with the head positioned in the Frankfort horizontal plane perpendicular to the floor. Our classification method was based on static MRI evaluation during which the head was in a neutral position to ensure consistent positioning during wakefulness; respiratory gating was not considered. The position of the velum would be expected to be affected by sedation, and the airway dimensions would be expected to be affected (to some extent) by the craniocervical inclination and respiration [22].

Second, measurements were made in three predetermined parallel planes; no visible genu was used to identify

Table 2 Definitions of parameters

Symbol	Type	Unit	Definition
Cross-sectional airway parameters			
latd	1D	mm	Lateral dimension of the airway at the A, B, and C planes
apd	1D	mm	Antero-posterior dimensions of the airway at the A, B, and C planes
R_1	Alatd/Aapd	Ratio	Ratio of airway lateral and AP dimensions at the A plane
R_2	Blatd/Bapd	Ratio	Ratio of airway lateral and AP dimensions at the B plane
R_3	Clatd/Capd	Ratio	Ratio of airway lateral and AP dimensions at the C plane
CSA	2D	mm^2	Cross-sectional areas of the airway at the A, B, and C planes
Midsagittal parameters			
L_1	1D	mm	Length from Ba to PNS (nasopharyngeal depth)
L_2	1D	mm	Length from ANS to PNS (hard palate length)
L_3	1D	mm	Length from Ba to ANS
L_4	1D	mm	Length from PNS to Val (pharyngeal length)
L_5	1D	mm	Length from PNS to UT (soft palate length)
L_6	1D	mm	Maximum soft palate thickness
L_7	1D	mm	Length from Mp to H
R_7	L_3/L_4	Ratio	Ratio of Ba-ANS to PNS-Val (vertical axis ratio)
α_1	Angular	°	OPT/NSL angle (craniocervical inclination)
α_2	Angular	°	N-S-Ba angle (cranial base angle)
α_3	Angular	°	ANS-PNS-Val angle
Cross-sectional soft tissue parameters			
L_8	1D	mm	Pharyngeal fat pad thickness at the B and C planes (bilaterally symmetrical)
L_9	1D	mm	Pharyngeal wall thickness at the B and C planes (bilaterally symmetrical)
Cross-sectional skeletal parameters			
L_{10}	1D	mm	Length between the mandibular medial borders of the B and C planes
L_{11}	1D	mm	Length from cv to fs at the B and C planes
L_{12}	1D	mm	Length between the CCs
L_{13}	1D	mm	Length between the Mpaps (maxilla width)
R_4	L_{12}/L_3	Ratio	Ratio of the lengths between the CCs and Ba-ANS (for the A plane)
R_5	L_{10}/L_{11}	Ratio	Ratio of craniofacial skeletal structural parameters at the B plane
R_6	L_{10}/L_{11}	Ratio	Ratio of craniofacial skeletal structural parameters at the C plane

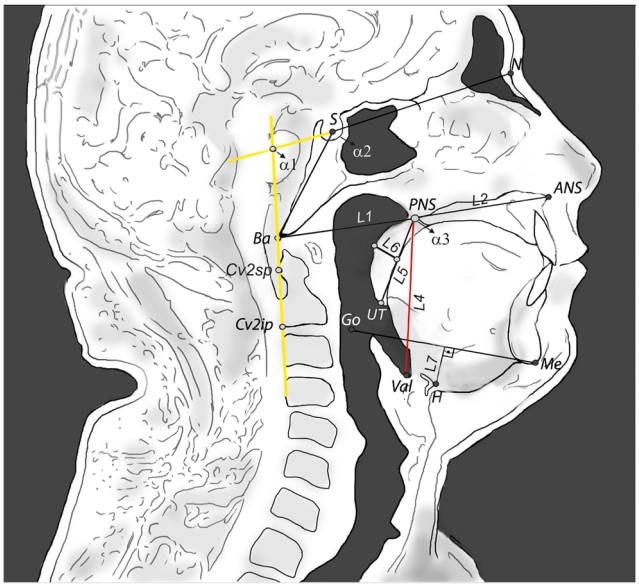

Fig. 2 Craniofacial landmarks: ANS, anterior nasal spine; PNS, posterior nasal spine; N, nasion; S, sella; H, most anterior point of the hyoid bone; Val; vallecula; Me, menton; Go, gonion; Ba, basion; UT, tip of the uvula. Measurements: L_1, BaPNS; L_2, ANS-PNS; L_3, Ba-ANS; L_4, PNS-Val; L_5, PNS-UT; L_6, maximum soft palate thickness; L_7, Mp-H: shortest distance between the mandibular plane (*Go-Me*) and H. Angles: α_1, OPT/NSL, angle between the tangent to the odontoid process that passes through *Cv2sp* (the superior posterior point of the second cervical vertebra) and *Cv2ip* (the inferior posterior point of the second cervical vertebra) and NSL (the nasion sella line); α_2, N-S-Ba, angle between NSL and the sella basion line; α_3, ANS-PNS-Val, angle between the ANS-PNS line and the PNS-Val line

intermediate patterns. We suggest that measurements on three predetermined proximal RP planes may provide reliable data regarding the baseline anatomical characteristics of a patient.

In addition, our method used a standard MRI protocol to analyze patients more objectively (thus without the bias of subjectively determining the genu).

Third, we lacked DISE data on our patients; we thus could not compare the MRI and DISE classification methods. DISE is indicated when surgery or placement of a mandibular repositioning device is being considered [23]. However, although DISE features direct dynamic imaging of upper airway structures, it does not yield quantitative data on the airway or the surrounding soft or hard tissues; metric evaluations or comparisons are not possible. MRI features indirect static evaluation of various structures, yielding quantitative data on both the airway and surrounding structures. It is true that MRI is expensive, but it should nonetheless be viewed as a powerful cost-effective tool.

Finally, our sample size was small, and the validity of our thresholds requires confirmation. Typical examples of the three types of RP patterns are shown in Fig. 4.

Cranial base, maxilla, and UAW soft tissue structures

Consistent with previous reports, a shorter nasopharyngeal depth (L_1) was evident in patients with the vertical pattern than the other patterns ($p < 0.001$) [12, 19, 24, 25]. In addition, a shorter hard palate length (L_2) and a smaller cranial base angle (α_2) were evident in those with the vertical pattern compared to others ($p = 0.03$, $p < 0.01$, respectively; Table 4). These data imply that the size and shape of the nasopharynx are determined in part by the cranial base and the osseous anatomy of the maxilla. Therefore, anteroposterior (L_3) narrowing at the palatal level reflects not only an anteroposteriorly restricted

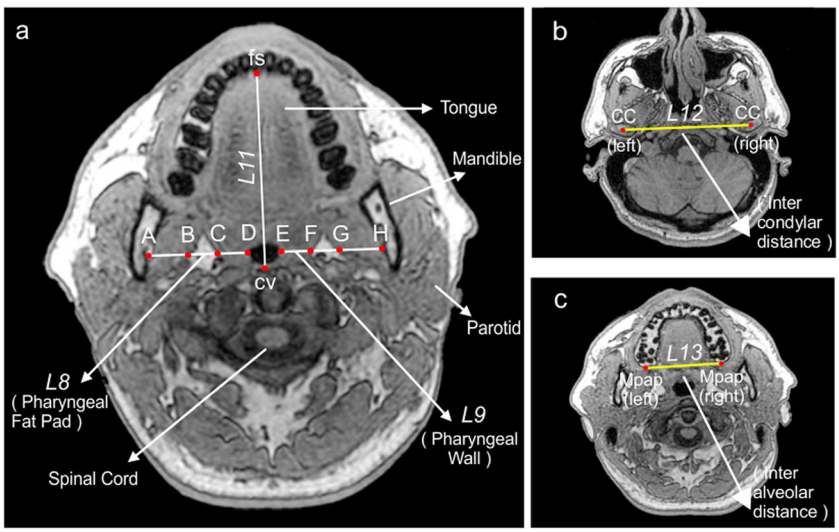

Fig. 3 **a** A representative T1-weighted axial MR image of the C plane. Important anatomical structures are labeled. The mandibular rami can be visualized by virtue of fat within the bone marrow of the mandible. L_8, pharyngeal fat pad thickness. B and C and F and G: L_9, pharyngeal wall thickness, C and D and E and F: L_{10}, intermandibular distance. A–H: L_{11}, the distance between *fs* (the facial skeletal border) and *cv* (the cervical vertebral border); **b** L_{12}, the intercondylar distance (the distance between the condyle centers *CC*); **c** L_{13}, the interalveolar distance (the distance between the midpoints of the ends of the tips of the alveolar process Mpap)

Table 3 Comparison of parameters by OSA category

No. of patients	AHI < 5 20	AHI 5 to < 15 18	AHI 15 to < 30 38	AHI 30 to < 50 18	AHI ≥ 50 23	*p*
Age (years)	40.05 ± 8.98[abcd]	44.33 ± 9.08[bc]	48.82 ± 10.33[d]	48.33 ± 8.55[d]	45.17 ± 8.6	0.01
AHI (events/h)	2.83 ± 1.56[abcd]	10.29 ± 3.2[bcd]	21.59 ± 4.78[cd]	38.85 ± 6.53[d]	64.63 ± 12.27	0.001
Min SaO_2 (%)	88.9 ± 2.4[cd]	85 ± 5.84[cd]	85.03 ± 3.75[cd]	81 ± 5.08[d]	73.91 ± 10.43	0.001
ST_{90} (min)	0.35 ± 0.46[abcd]	1.99 ± 3.04[bcd]	4.96 ± 7.74[cd]	20.55 ± 23.47[d]	64.29 ± 74.07	0.001
ESS	8.2 ± 4.41	9.61 ± 5.65	10.97 ± 5.24	11.33 ± 4.77	9.65 ± 5.59	NS
BMI (kg/m^2)	27.19 ± 3.65[abcd]	30.32 ± 3.59	29.6 ± 3.39	29.96 ± 2.98	31.08 ± 3.95	0.01
Cross-sectional airway parameters						
Alatd	24.39 ± 4.06[abcd]	20.68 ± 3.75	22.16 ± 3.68	20.93 ± 3.15	21.63 ± 3.76	0.02
Aapd	18.8 ± 3.09	18.37 ± 3.31	17.39 ± 3.74	17.12 ± 2.05	16.85 ± 3.51	NS
Blatd	20.05 ± 5.6[abcd]	15.66 ± 4.54	15.93 ± 4.15	15.1 ± 4.97	15.59 ± 4.4	0.01
Bapd	9.78 ± 2.59	10.49 ± 2.75	10.7 ± 2.5	9.93 ± 2.2	10.7 ± 2.63	NS
Clatd	17.82 ± 5.45[abcd]	14.44 ± 5.86	13.94 ± 5.08	13.71 ± 5.85	12.64 ± 5.24	0.032
Capd	6.35 ± 2.07[d]	6.88 ± 2.62[d]	6.9 ± 1.81[d]	6.11 ± 1.5[d]	7.27 ± 2.1	0.035
R_1	1.32 ± 0.26	1.15 ± 0.24	1.34 ± 0.4	1.23 ± 0.17	1.36 ± 0.52	NS
R_2	2.22 ± 0.97[abcd]	1.53 ± 0.42	1.53 ± 0.45	1.55 ± 0.43	1.57 ± 0.74	0.001
R_3	3.16 ± 1.52[abcd]	2.39 ± 1.46[d]	2.18 ± 1.12	2.3 ± 0.89	1.99 ± 1.36	0.035
CSA at A	502.96 ± 124.69[abcd]	405.09 ± 119.52[bd]	441.68 ± 111.51[cd]	406.08 ± 104.38[d]	393.56 ± 92.56	0.01
CSA at B	168.28 ± 56.56	144.68 ± 72.43	151.7 ± 64.07	138.53 ± 70.97	141.28 ± 46	NS
CSA at C	103.15 ± 47.22	95.83 ± 72.41	89.63 ± 43.3	77.56 ± 51.97	81.55 ± 36	NS
Midsagittal parameters						
L_1	41.87 ± 4.47	41.1 ± 3.35	40.5 ± 3.59	40.82 ± 3.16	40 ± 3.91	NS
L_2	57.02 ± 2.89	56.47 ± 5.73	56.93 ± 3.54	56.48 ± 4.62	55.27 ± 3.08	NS
L_3	98.45 ± 5.78	97.18 ± 6.08	97.24 ± 5.44	97.54 ± 5.22	96.17 ± 6.2	NS
L_4	73.28 ± 7.96[d]	71.6 ± 6.54[d]	75.77 ± 7.34[d]	76.64 ± 5.7[d]	78.86 ± 5.73	0.01
L_5	39.24 ± 3.57[abcd]	39.23 ± 3.98[bcd]	41.75 ± 3.59	41.14 ± 2.89	42.24 ± 4.01	0.013
L_6	10.38 ± 1.02[cd]	10 ± 1.57[cd]	10.68 ± 1.53	11.51 ± 1.53	11.42 ± 1.8	0.01
L_7	20.47 ± 6.62[cd]	20.32 ± 4.67[cd]	22.93 ± 5.64[d]	24.18 ± 5.19[d]	28.17 ± 4.18	0.001
R_7	1.36 ± 0.19[cd]	1.37 ± 0.17[cd]	1.3 ± 0.17[cd]	1.28 ± 0.1	1.23 ± 0.13	0.02
α_1	101.83 ± 6.7	100.56 ± 5.39	101.5 ± 6.2	102.91 ± 6.18	104.68 ± 4.61	NS
α_2	127.06 ± 5.41	126.59 ± 4.48	125.56 ± 6.13	126.02 ± 8.15	126.3 ± 5.44	NS
α_3	102.94 ± 5.66	102.59 ± 6.22	101.08 ± 4.93	103.85 ± 5.46	103.1 ± 4.36	NS
Cross-sectional soft tissue parameters						
L_8 at B	7.16 ± 2.15	7.94 ± 2.95	7.88 ± 3.22	8.01 ± 3.57	8.12 ± 2.57	NS
L_8 at C	9.3 ± 3.71	9.02 ± 2.36	9.92 ± 2.92	9.91 ± 2.91	9.6 ± 2.8	NS
L_9 at B	7.59 ± 1.62	7.86 ± 1.9	7.87 ± 1.95	8.76 ± 2.75	8.02 ± 2.35	NS
L_9 at C	11.61 ± 2.69	11.36 ± 1.97	11.38 ± 2.81	11.09 ± 3.29	12.29 ± 3.99	NS
Cross-sectional skeletal parameters						
L_{10} at B	93.41 ± 4.6	94.79 ± 6.45	94.78 ± 5.46	94.48 ± 4.36	94.03 ± 4.07	NS
L_{10} at C	93.41 ± 4.08	92.59 ± 5.4	92.26 ± 5.29	93.18 ± 4.02	92.5 ± 4.46	NS
L_{11} at B	65 ± 5.42	66.97 ± 5.88	65.21 ± 5.62	66.57 ± 5.2	66.8 ± 6.19	NS
L_{11} at C	75.5 ± 7.14	75.62 ± 6.65	74.62 ± 5.97	76.12 ± 7.17	75.64 ± 6.17	NS
L_{12}	105.25 ± 6.18	105.24 ± 7.61	107.11 ± 6.68	107.56 ± 6.39	107.11 ± 4.91	NS
L_{13}	48.52 ± 3.99	47.81 ± 3.19	47.78 ± 3.08	46.76 ± 3.96	47.69 ± 3.44	NS
R_4	1.07 ± 0.1	1.09 ± 0.1	1.1 ± 0.09	1.11 ± 0.11	1.12 ± 0.1	NS
R_5	1.45 ± 0.15	1.42 ± 0.15	1.46 ± 0.13	1.43 ± 0.12	1.42 ± 0.14	NS
R_6	1.25 ± 0.13	1.23 ± 0.13	1.24 ± 0.11	1.23 ± 0.1	1.23 ± 0.1	NS

Data are means ± standard deviations, numbers of subjects (%)

Other abbreviations as in Table 2

AHI, apnea-hypopnea index; *min SaO_2*, lowest oxygen saturation; *ST_{90}*, total sleep time with oxygen saturation < 90%; *ESS*, Epworth sleepiness scale; *BMI*, body mass index; *NS*, not significant

[a] Different between AHI 5 and < 15

[b] Different between AHI 15 and < 30

[c] Different between AHI 30 and < 50

[d] Different from AHI ≥ 50

maxilla but also a narrow cranial base angle. A longer pharynx (L_4) was also evident in patients with the vertical pattern. Finkelstein et al. reported that posterior insertion of the velar muscles into the cranial base results in a flatter, laterally larger velopharyngeal axial configuration [25]. However, Enlow stated that a regional imbalance often tends to compensate, providing functional equilibrium [26]. Together, these findings suggest that to fit into the anteroposteriorly restricted cranial base

Table 4 Comparison of parameters by retropalatal pattern group

	Oblique	Vertical	Intermediate	
No. of patients (%)	50 (43)	24 (20)	43 (37)	*p*
Age (years)	47.1 ± 8.23	41.83 ± 11.37	46.6 ± 9.93	NS
AHI (events/h)	31.37 ± 22.61[b]	33.48 ± 26.13[b]	20.38 ± 17.88	0.02
Min SaO_2 (%)	81.22 ± 8.87	83.58 ± 6.01	84.42 ± 6.89	NS
ST_{90} (min)	27.8 ± 57.48	11.08 ± 24.63	9.86 ± 18.6	NS
ESS	9.9 ± 4.7	11.13 ± 5.46	9.72 ± 5.64	NS
BMI (kg/m^2)	30.69 ± 2.97[a]	27.77 ± 4.58[b]	29.48 ± 3.5	0.001
Cross-sectional airway parameters				
Alatd	20.38 ± 3.2[ab]	25.03 ± 4.21	22.25 ± 3.24	0.001
Aapd	18.18 ± 2.82[a]	14.51 ± 3.63[b]	18.75 ± 2.63	0.001
Blatd	13.45 ± 3.13[ab]	18.86 ± 5.63	18.46 ± 4.32	0.001
Bapd	11.5 ± 2.16[ab]	9.45 ± 2.7	9.63 ± 2.36	0.001
Clatd	11.07 ± 3.66[ab]	17.69 ± 6.93	16.4 ± 4.52	0.001
Capd	7.6 ± 1.8[ab]	6.39 ± 2.49	5.97 ± 1.6	0.001
R_1	1.14 ± 0.18[a]	1.8 ± 0.46[b]	1.2 ± 0.16	0.001
R_2	1.17 ± 0.2[ab]	2.07 ± 0.7	2 ± 0.64	0.001
R_3	1.48 ± 0.42[ab]	3.15 ± 1.71	2.94 ± 1.13	0.001
CSA at A	401.16 ± 104.12[ab]	423.63 ± 129.38[b]	471.42 ± 109.44	0.01
CSA at B	134.22 ± 48.11	163.34 ± 89.84	159.21 ± 54.78	NS
CSA at C	79.58 ± 38.66	102.2 ± 73.69	93.8 ± 42.55	NS
Midsagittal parameters				
L_1	41.83 ± 3.33[a]	37.62 ± 3.56[b]	41.32 ± 3.29	0.001
L_2	57.23 ± 3.93[a]	54.62 ± 3.99[b]	56.65 ± 3.67	0.03
L_3	99.35 ± 5.08[a]	91.43 ± 5.04[b]	98.11 ± 4.39	0.001
L_4	75.68 ± 6.53[a]	82.19 ± 4.53[b]	71.4 ± 5.98	0.001
L_5	41.18 ± 3.93	40.65 ± 3.98	40.81 ± 3.56	NS
L_6	11.14 ± 1.46	10.49 ± 1.95	10.57 ± 1.47	NS
L_7	23.9 ± 5.79[ab]	27.11 ± 4.77[b]	20.55 ± 5.46	0.001
R_7	1.32 ± 0.14[a]	1.11 ± 0.07[b]	1.38 ± 0.15	0.001
α_1	102.7 ± 5.63	101.4 ± 6.21	102.22 ± 6.25	NS
α_2	127.71 ± 4.68[a]	123.42 ± 6.59[b]	125.98 ± 6.42	0.01
α_3	102.49 ± 4.18[a]	100.06 ± 5.39[b]	103.75 ± 5.93	0.02
Cross-sectional soft tissue parameters				
L_8 at B	8.27 ± 2.83[a]	6.23 ± 2.65[b]	8.22 ± 2.93	0.01
L_8 at C	10.43 ± 2.79[a]	8.13 ± 2.05[b]	9.48 ± 3.22	0.01
L_9 at B	8.37 ± 2.56	8.02 ± 1.81	7.52 ± 1.57	NS
L_9 at C	11.94 ± 3.17	11.3 ± 3.17	11.23 ± 2.71	NS
Cross-sectional skeletal parameters				
L_{10} at B	95 ± 4.84	94.39 ± 4.92	93.58 ± 5.3	NS
L_{10} at C	92.76 ± 4.63	92.44 ± 4.69	92.77 ± 4.94	NS
L_{11} at B	67.94 ± 4.97[a]	60.58 ± 5.42[b]	66.67 ± 4.64	0.001
L_{11} at C	77.57 ± 4.98[a]	68.41 ± 5.92[b]	76.65 ± 5.53	0.001
L_{12}	106.59 ± 6.68	108.57 ± 5.55	105.44 ± 6.25	NS
L_{13}	47.65 ± 3.31	47.21 ± 3.67	48.13 ± 3.53	NS
R_4	1.08 ± 0.09[a]	1.19 ± 0.09[b]	1.08 ± 0.08	0.001
R_5	1.4 ± 0.11[a]	1.57 ± 0.15[b]	1.41 ± 0.12	0.001
R_6	1.2 ± 0.09[a]	1.36 ± 0.11[b]	1.21 ± 0.09	0.001

Data are means ± standard deviations, numbers of subjects (%)

Other abbreviations as in Table 2

AHI, apnea-hypopnea index; *min SaO_2*, lowest oxygen saturation; *ST_{90}*, total sleep time with oxygen saturation < 90%; *ESS*, Epworth sleepiness scale; *BMI*, body mass index; *NS*, not significant

[a] Different from the vertical group

[b] Different from the intermediate group

area in individuals with a narrow α_2 angle, the velar muscles insert more posteriorly into the cranial base and are oriented more vertically; thus, the longitudinal curvature increases and the pharyngeal airway flattens anteroposteriorly and may be elongated inferiorly as a compensatory mechanism. The ANS-PNS-Val angle (α_3) was measured as an indicator of longitudinal curvature; the mean value was lower in those with the vertical pattern ($p = 0.02$). In addition, a moderate correlation was evident between the craniocervical inclination (α_1) and the longitudinal curvature (α_3; $r = 0.504$, $p < 0.001$). In contrast to those with the vertical pattern, our findings suggest that in those with the oblique pattern, the cranial base area narrows laterally and the velar muscles are inserted more laterally into the cranial base and are also oriented more anteroposteriorly.

Table 5 Distribution of retropalatal patterns by OSA category

	AHI < 5	AHI 5 to < 15	AHI 15 to < 30	AHI 30 to < 50	AHI ≥ 50	*p*
Oblique	3[abd] (6)	10 (20)	17 (34)	7 (14)	13 (26)	0.049
Vertical	4[bd] (17)	2[bd] (8)	9 (38)	3 (13)	6 (25)	
Intermediate	13[abd] (30)	6[b] (14)	12[d] (28)	8 (19)	4 (9)	

Data are numbers of subjects (%)

[a] Different between AHI 5 and < 15

[b] Different between AHI 15 and < 30

[c] Different between AHI 30 and < 50

[d] Different from AHI ≥ 50

However, our findings suggest that in those with the intermediate pattern the cranial base area is large in the lateral and AP dimensions and, as a result, pharyngeal length is shortened vertically. OSA is an adverse consequence of human upper respiratory tract evolution, because during the development of a newborn, not only is an adequate distance between the epiglottis and soft palate required for speech, but closure for deglutition without aspiration should also be maintained. A good balance between maxillary development and laryngeal descent is important in this complex process [27, 28]. Therefore, increased velar angulation (genu formation) in patients with an intermediate pattern may be a compensatory mechanism associated with a short pharynx.

The etiology of hyoid displacement

Significant differences in the Mp-H (L_7) distance were evident among the three groups ($p < 0.001$; Table 4). A longer Mp-H distance indicates a longer (and therefore more collapsible) soft tissue pharyngeal airway, which is associated with poorer UPPP outcomes [29–31]. Consistent with this, a moderate correlation was apparent between pharyngeal length and Mp-H distance ($r = 0.680$, $p < 0.001$). Excessive soft tissue may shift the hyoid bone caudally; similarly, a relative excess of soft tissue in patients with a small mandibular enclosure may cause a downward shift of the hyoid bone in nonobese individuals [24, 32]. This means that the Mp-H distance may be increased in patients with all of the RP patterns studied. Our findings suggest that the Mp-H distance is determined in part by the type of RP pattern, obesity, and the extent of contiguous soft tissue structures.

Correlations between the cross-sectional shape and the vertical axis

One airway ratio (R_1) and all three skeletal ratios (R_4, R_5, R_6) were significantly (negatively) correlated with the vertical axis ratio (R_7; Table 7). These findings suggest that the RP airway pattern is associated not only with bony enclosures in the cross-sectional plane but also with pharyngeal length in the vertical plane in all three dimensions. Linear regression analyses revealed that 40.8% of the variance in the vertical axis ratio was predicted by the R_1 ratio and the A, B, and C skeletal ratios ($p < 0.001$; Table 8).

Table 6 Simple and partial correlations between airway and skeletal ratios

		R_4 *r* (p)	R_5 *r* (p)	R_6 *r* (p)
R_1	[a]	0.353 (< 0.001)	0.337 (< 0.001)	0.384 (< 0.001)
	[b]	0.356 (< 0.001)	0.296 (< 0.001)	0.348 (< 0.001)
R_2	[a]	0.130 (NS)	0.212 (NS)	0.313 (< 0.001)
	[b]	0.048 (NS)	0.09 (NS)	0.190 (0.042)
R_3	[a]	0.220 (< 0.001)	0.332 (< 0.001)	0.397 (< 0.001)
	[b]	0.147 (NS)	0.251 (0.007)	0.299 (< 0.001)

Abbreviations as in Table 2

NS, not significant

[a] Unadjusted correlations

[b] Correlations adjusted for BMI and age

Table 7 Simple and partial correlations between cross-sectional and vertical axis ratios

	R_7 *r* (p)	R_7 (adjusted for BMI, age, and OPT/NSL) *r* (p)
R_1	− 0.404 (< 0.001)	− 0.427 (0.001)
R_2	− 0.271 (0.003)	− 0.144 (NS)
R_3	− 0.264 (0.004)	− 0.177 (NS)
R_4	− 0.731 (< 0.001)	− 0.569 (0.001)
R_5	− 0.503 (0.001)	− 0.433 (0.001)
R_6	− 0.518 (< 0.001)	− 0.502 (< 0.001)

Abbreviations as in Table 2

NS, not significant

Table 8 Change in the corrected vertical axis ratio (R_7) per unit of R_1, R_4, R_5, and R_6

	Change in R_7 per unit increase in …					
	R_1	R_4	R_5	R_6	R^2	*F* ANOVA test *p* value
R_7	− 0.098 (0.007)	− 0.660 (0.001)	0.092 (NS)	− 0.364 (0.049)	0.408	< 0.001

Abbreviations as in Table 2

NS, not significant

The effect of age and RP pattern on pharyngeal caliber

A previous study reported that compared to younger males older males had a greater pharyngeal caliber as measured by acoustic reflection, a longer and larger soft palate and parapharyngeal fat pad (measured using MRI); this study concluded that the larger pharyngeal caliber observed in older males may compensate for the age-related enlargement of the pharyngeal soft tissue that predisposes one to OSA [33]. A correlation was evident between the airway and skeletal ratios at the A plane (Table 6). This reflects a relationship between the airway anterior-posterior length and the nasopharyngeal depth (BaPNS). The positive correlations between the airway and skeletal ratios at the A plane fell at lower planes (Table 6), possibly because of the extent of soft tissue increases from the hard palate to the lower levels. Indeed, the mean pharyngeal fat pad thicknesses at the B and C planes were significantly lower in patients with the vertical pattern than others (Table 4). These data suggest that compensatory mechanisms affording functional equilibrium are dynamic, in play not only in childhood but also in adulthood, mediated by changes in the sizes and configurations of adjacent soft tissues [25, 26, 33].

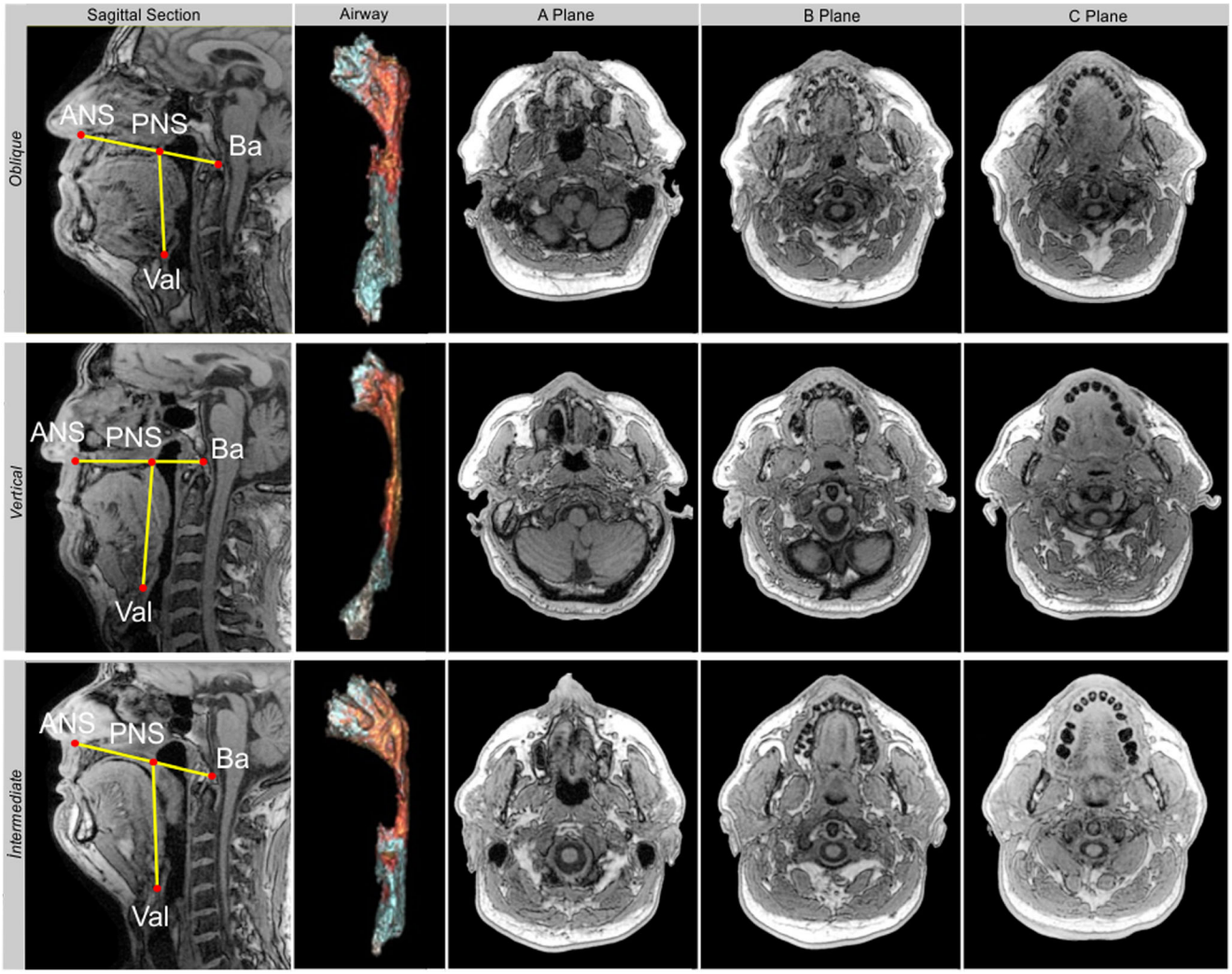

Fig. 4 Magnetic resonance images of patients with oblique (first row), vertical (second row), and intermediate (third row) retropalatal patterns. ANS, anterior nasal spine; PNS, posterior nasal spine; Ba, basion; Val, vallecula. Images show the midsagittal section, 3D airway (lateral view), cross-section of A, B, C planes of each patient, respectively. ANS, anterior nasal spine; PNS, posterior nasal spine; Ba, basion; Val, vallecula

Factors limiting the effect of oral appliances and upper airway stimulation

The resolution of a multilevel collapse of the palate and tongue base is probably critical if treatment is to succeed [10]. Increases after stimulation in the anteroposterior RP dimension, and the anteroposterior and lateral retrolingual dimensions, may indicate that an additive mechanism differing from that of oral appliances is in play [9, 34]. Anatomically, the soft palate is linked to the tongue base via the anterior palatal pillar, which contains the palatoglossus muscle that courses through the soft palate and uvula and inserts into the sides of the tongue [35]. This structure can passively and actively pull the soft palate inferiorly and anteriorly.

The connection between hypoglossal activation and upper airway structural movement, and the passive effect of tongue-base manipulation during mandibular advancement, followed by RP opening, deserve further investigation [10]. We suggest that the effects of mandibular advancement and stimulation on the upper airway are associated with the RP pattern. These patterns differ not only in terms of airway size and shape but also in the insertion sites and orientations of the pharyngeal muscles, influencing the muscle responses to all treatment modalities.

Factors potentially limiting surgical success

Our findings may be relevant from a surgical point of view. Surgical success or failure is dependent on accurate airway diagnosis and selection of the correct procedure [12]. According to our results, the baseline anatomy not only pertains to surgically removable or alterable soft tissue structures but also involves a narrow cranial base angle, a narrow nasopharynx, an anteroposteriorly restricted maxilla, abnormally inserted and oriented velar muscles, and abnormal pharyngeal length, which cannot be addressed adequately by surgery; these factors may limit surgical success. UPPP, palatal advancement, and/or lateral pharyngoplasty would not be expected to adequately address abnormalities associated with the cranial base, muscle insertion or orientation, or pharyngeal length. Furthermore, the overall space available to accommodate upper airway soft tissue is genetically determined [36]. Our results suggest that the vertical pattern is associated with a narrow cranial base angle, a short nasopharynx, and a long pharynx; the oblique pattern is associated with narrow nasopharyngeal lateral dimensions; and the intermediate pattern is associated with large nasopharyngeal dimensions and a short pharynx. All patterns may be heritable. These findings support the hypothesis that anatomical imbalances may be best treated by orthodontic treatments following early diagnosis during the developmental period [37].

After maxillomandibular and genial tubercle advancement, the upper airway became shorter in length but larger in size (in terms of both volume and the CSA), and more uniform, more closely resembling a normal airway [38]. In the present study, a large CSA at A and a short airway length were characteristic of patients with the intermediate pattern. Also, of OSA patients, the percentages of those with the oblique, vertical, and intermediate RP patterns were 94, 83, and 70%, respectively ($p = 0.049$), implying that a tendency toward OSA is relatively high in those with the oblique pattern, moderate in those with the vertical pattern, and low in those with the intermediate pattern (Table 5). We speculate that the vertical pattern transforms into an intermediate pattern to some extent after maxillomandibular and genial tubercle advancement. However, even this highly invasive surgical procedure does not adequately address an abnormally sized/shaped cranial base, or muscle insertion and orientation. OSA recurrences have been noted 10–15 years after maxillomandibular advancement. One of the limitations of such surgery (observed clinically in many recurrences) is the limited gain in the lateral dimension of the pharyngeal airway, despite good long-term gain in the anteroposterior direction [39].

Future research perspectives

Pharmacotherapy for nonanatomical traits must move from proof-of-principle to the clinic. Similarly, the roles of novel devices must be better defined. For example, how do the devices manipulate the airway? What is the magnitude of their effect? Further, which patients best respond to such therapies [40]?

It is unknown whether loop gain and the arousal threshold influence upper airway size [5], or vice versa. No standardized quantitative classification of UAW anatomical traits is yet available. An important objective of future research should be clarification of the relative contributions of, and interactions among, the abovementioned factors (anatomical and nonanatomical) in terms of OSA development [41, 42]. The surgical reduction of upper airway collapsibility may be related to the baseline anatomical features of the patient (i.e., the obstruction sites and structural components involved in a collapse). Nonanatomical traits such as a high loop gain and arousal threshold are associated with residual AHI after upper airway surgery. However, an understanding of OSA physiology, rather than a reliance on unguided statistical methods, is necessary in order to use anatomical and nonanatomical surrogates of physiological traits to predict surgical outcomes [43].

We suggest that the responses to various OSA therapies may be associated with RP patterns. If so, accurate anatomical information obtained before and after surgery is crucial to aid our understanding of OSA pathophysiology and evaluation of the responses to different modalities. It should be emphasized that an endoscopically visible genu is not a reliable landmark when used to differentiate patients with intermediate RP patterns. Patients with vertical RP patterns may be distinguished more readily, but oblique and intermediate patterns can be

confused on endoscopy. The oblique and intermediate RP patterns reflect the two ends of the spectrum regarding the CSA at A; and the vertical axis ratio of the vertical pattern differ significantly from those in other patterns. The obstruction sites and structural components of collapse may be more important than isolated, pharyngeal critical pressures. Future work on RP patterns will aid our understanding of OSA pathogenesis and may result in the development of new, effective treatment strategies.

In conclusion, our study, which used MRI to examine craniofacial structures in patients with simple snoring and OSA, measured the RP airways of male patients three-dimensionally and quantitatively. Anatomical imbalances related to nasopharyngeal dimensions and pharyngeal length, and compensatory processes providing functional equilibrium, may contribute to baseline anatomical characteristics of the RP airway. An awareness of these associations will improve the ability of physicians to understand and interpret multiple airway patterns and could guide decisions on appropriate treatment modalities.

Funding This study was supported by the Baskent University Research Fund (project no. KA17/36).

Compliance with ethical standards

Conflict of interest The authors declare that they have no conflict of interest.

Ethical approval All procedures involving human participants were performed in accordance with the ethical standards of our institutional and/or national research committee and with those of the 1964 Helsinki declaration and later amendments, or comparable ethical standards.

Informed consent Informed consent was obtained from all participants.

References

1. White DP, Younes MK (2012) Obstructive sleep apnea. Compr Physiol 2:2541–2594. https://doi.org/10.1002/cphy.c110064
2. Eckert DJ, White DP, Jordan AS, Malhotra A, Wellman A (2013) Defining phenotypic causes of obstructive sleep apnea. Identification of novel therapeutic targets. Am J Respir Crit Care Med 188:996–1004. https://doi.org/10.1164/rccm.201303-0448OC
3. Eckert DJ (2018) Phenotypic approaches to obstructive sleep apnoea—new pathways for targeted therapy. Sleep Med Rev 37:45–59. https://doi.org/10.1016/j.smrv.2016.12.003
4. Carberry JC, Amatoury J, Eckert DJ (2018) Personalized management approach for OSA. Chest 153:744–755. https://doi.org/10.1016/j.chest.2017.06.011
5. Chen H, Aarab G, de Ruiter MH, de Lange J, Lobbezoo F, van der Stelt PF (2016) Three-dimensional imaging of the upper airway anatomy in obstructive sleep apnea: a systematic review. Sleep Med 21:19–27. https://doi.org/10.1016/j.sleep.2016.01.022
6. Chai-Coetzer CL, Antic NA, Rowland LS, Reed RL, Esterman A, Catcheside PG, Eckermann S, Vowles N, Williams H, Dunn S, McEvoy RD (2013) Primary care vs specialist sleep center management of obstructive sleep apnea and daytime sleepiness and quality of life: a randomized trial. JAMA 309:997–1004. https://doi.org/10.1001/jama.2013.1823
7. Trudo FJ, Gefter WB, Welch KC, Gupta KB, Maislin G, Schwab RJ (1998) State-related changes in upper airway caliber and surrounding soft-tissue structures in normal subjects. Am J Respir Crit Care Med 158:1259–1270
8. Leiter JC (1996) Upper airway shape: is it important in the pathogenesis of obstructive sleep apnea? Am J Respir Crit Care Med 153:894–898
9. Chan AS, Lee RW, Srinivasan VK, Darendeliler MA, Grunstein RR, Cistulli PA (2010) Nasopharyngoscopic evaluation of oral appliance therapy for obstructive sleep apnoea. Eur Respir J 35:836–842. https://doi.org/10.1183/09031936.00077409
10. Safiruddin F, Vanderveken OM, de Vries N, Maurer JT, Lee K, Ni Q, Strohl KP (2015) Effect of upper-airway stimulation for obstructive sleep apnoea on airway dimensions. Eur Respir J 45:129–138. https://doi.org/10.1183/09031936.00059414
11. Pang KP, Woodson BT (2013) Current concepts in evaluation and surgical planning: the Pang–Woodson protocol. In: Pang KP, Woodson BT, Rotenberg B (eds) Advanced surgical technique in snoring and obstructive sleep apnea, 1st edn. Plural Publishing, USA, pp 37–42
12. Woodson BT (2008) Structural effectiveness of pharyngeal sleep apnea surgery. Sleep Med Rev 12:463–479. https://doi.org/10.1016/j.smrv.2008.07.010
13. Li HY, Chen NH, Wang CR, Shu YH, Wang PC (2003) Use of 3-dimensional computed tomography scan to evaluate upper airway patency for patients undergoing sleep-disordered breathing surgery. Otolaryngol Head Neck Surg 129:336–342. https://doi.org/10.1016/S0194-59980300629-6
14. Ryan CF, Lowe AA, Li D, Fleetham JA (1991) Three-dimensional upper airway computed tomography in obstructive sleep apnea. A prospective study in patients treated by uvulopalatopharyngoplasty. Am Rev Respir Dis 144:428–432. https://doi.org/10.1164/ajrccm/144.2.428
15. Cahali MB, Formigoni GG, Gebrim EM, Miziara ID (2004) Lateral pharyngoplasty versus uvulopalatopharyngoplasty: a clinical, polysomnographic and computed tomography measurement comparison. Sleep 27:942–950
16. Denolf PL, Vanderveken OM, Marklund ME, Braem MJ (2016) The status of cephalometry in the prediction of non-CPAP treatment outcome in obstructive sleep apnea patients. Sleep Med Rev 27:56–73. https://doi.org/10.1016/j.smrv.2015.05.009
17. Woodson BT (2015) A method to describe the pharyngeal airway. Laryngoscope 125:1233–1238. https://doi.org/10.1002/lary.24972
18. Woodson BT, Sitton M, Jacobowitz O (2012) Expansion sphincter pharyngoplasty and palatal advancement pharyngoplasty: airway evaluation and surgical techniques. Oper Tech Otolaryngol Head Neck Surg 23:3–10. https://doi.org/10.1016/j.otot.2012.01.002
19. Woodson BT (2013) Palatal advancement pharyngoplasty. In: Pang KP, Woodson BT, Rotenberg B (eds) Advanced surgical technique in snoring and obstructive sleep apnea, 1st edn. Plural Publishing, USA, pp 167–177
20. Iber C, Ancoli-Israel S, Chesson A, Quan S (2007) The AASM manual for the scoring of sleep and associated events: rules, terminology and technical specifications. American Academy of Sleep Medicine, Westchester
21. Berry RB, Budhiraja R, Gottlieb DJ, Gozal D, Iber C, Kapur VK, Marcus CL, Mehra R, Parthasarathy S, Quan SF, Redline S, Strohl KP, Ward SLD, Tangredi MM (2012) Rules for scoring respiratory events in sleep: update of the 2007 AASM manual for the scoring of sleep and associated events. J Clin Sleep Med 8:597–619. https://doi.org/10.5664/jcsm.2172
22. Muto T, Takeda S, Kanazawa M, Yamazaki A, Fujiwara Y, Mizoguchi I (2002) The effect of head posture on the pharyngeal

airway space (PAS). Int J Oral Maxillofac Surg 31:579–583. https://doi.org/10.1016/j.ijom.2007.12.012
23. Abdullah VJ, Koutsourelakis I, Ravesloot MJL, Lip Yen Lee D, Ching Nam Ha S, van Hasselt CA et al (2013) Drug-induced sleep endoscopy. In: Pang KP, Woodson BT, Rotenberg B (eds) Advanced surgical technique in snoring and obstructive sleep apnea, 1st edn. Plural Publishing, USA, pp 43–65
24. Watanabe T, Isono S, Tanaka A, Tanzawa H, Nishino T (2002) Contribution of body habitus and craniofacial characteristics to segmental closing pressures of the passive pharynx in patients with sleep-disordered breathing. Am J Respir Crit Care Med 165:260–265. https://doi.org/10.1164/ajrccm.165.2.2009032
25. Finkelstein Y, Shapiro-Feinberg M, Talmi YP, Nachmani A, DeRowe A, Ophir D (1995) Axial configuration of the velopharyngeal valve and its valving mechanism. Cleft Palate Craniofac J 32:299–305. https://doi.org/10.1597/1545-1569(1995)032<0299:ACOTVV>2.3.CO;2
26. Enlow DH (1982) Handbook of facial growth, 2nd edn. WB Saunders Company, Philadelphia
27. Davidson TM (2003) The great leap forward: the anatomic basis for the acquisition of speech and obstructive sleep apnea. Sleep Med 4:185–194
28. Yamashiro Y, Kryger M (2012) Is laryngeal descent associated with increased risk for obstructive sleep apnea? Chest 141:1407–1413. https://doi.org/10.1378/chest.10-3238
29. Woodson BT, Conley SF (1997) Prediction of uvulopalatopharyngoplasty response using cephalometric radiographs. Am J Otolaryngol 18:179–184
30. Doghramji K, Jabourian ZH, Pilla M, Farole A, Lindholm RN (1995) Predictors of outcome for uvulopalatopharyngoplasty. Laryngoscope 105:311–314. https://doi.org/10.1288/00005537-199503000-00016
31. Millman RP, Carlisle CC, Rosenberg C, Kahn D, McRae R, Kramer NR (2000) Simple predictors of uvulopalatopharyngoplasty outcome in the treatment of obstructive sleep apnea. Chest 118:1025–1309
32. Genta PR, Schorr F, Eckert DJ, Gebrim E, Kayamori F, Moriya HT, Malhotra A, Lorenzi-Filho G (2014) Upper airway collapsibility is associated with obesity and hyoid position. Sleep 37:1673–1678. https://doi.org/10.5665/sleep.4078
33. Carlisle T, Carthy ER, Glasser M, Drivas P, McMillan A, Cowie MR, Simonds AK, Morrell MJ (2014) Upper airway factors that protect against obstructive sleep apnoea in healthy older males. Eur Respir J 44:685–693. https://doi.org/10.1183/09031936.00177213
34. Chan AS, Sutherland K, Schwab RJ, Zeng B, Petocz P, Lee RW, Darendeliler MA, Cistulli PA (2010) The effect of mandibular advancement on upper airway structure in obstructive sleep apnoea. Thorax 65:726–732. https://doi.org/10.1136/thx.2009.131094
35. Van de Graaff WB, Gottfried SB, Mitra J, van Lunteren E, Cherniack NS, Strohl KP (1984) Respiratory function of hyoid muscles and hyoid arch. J Appl Physiol Respir Environ Exerc Physiol 57:197–204
36. Chi L, Comyn FL, Keenan BT, Cater J, Maislin G, Pack AI, Schwab RJ (2014) Heritability of craniofacial structures in normal subjects and patients with sleep apnea. Sleep 37:1689–1698
37. Huynh NT, Desplats E, Almeida FR (2016) Orthodontics treatments for managing obstructive sleep apnea syndrome in children: a systematic review and meta-analysis. Sleep Med Rev 25:84–94
38. Abramson Z, Susarla SM, Lawler M, Bouchard C, Troulis M, Kaban LB (2011) Three-dimensional computed tomographic airway analysis of patients with obstructive sleep apnea treated by maxillomandibular advancement. J Oral Maxillofac Surg 69:677–686. https://doi.org/10.1016/j.joms.2010.11.037
39. Zaghi S, Holty JE, Certal V, Abdullatif J, Guilleminault C, Powell NB et al (2016) Maxillomandibular advancement for treatment of obstructive sleep apnea: a meta-analysis. JAMA Otolaryngol Head Neck Surg 142:58–66. https://doi.org/10.1001/jamaoto.2015.2678
40. Malhotra A, Orr JE, Owens RL (2015) On the cutting edge of obstructive sleep apnoea: where next? Lancet Respir Med 3:397–403. https://doi.org/10.1016/S2213-2600(15)00051-X
41. Chi L, Comyn FL, Mitra N, Reilly MP, Wan F, Maislin G, Chmiewski L, Thorne-FitzGerald MD, Victor UN, Pack AI, Schwab RJ (2011) Identification of craniofacial risk factors for obstructive sleep apnoea using three-dimensional MRI. Eur Respir J 38:348–358. https://doi.org/10.1183/09031936.00119210
42. Owens RL, Edwards BA, Eckert DJ, Jordan AS, Sands SA, Malhotra A, White DP, Loring SH, Butler JP, Wellman A (2015) An integrative model of physiological traits can be used to predict obstructive sleep apnea and response to non positive airway pressure therapy. Sleep 38:961–970
43. Li Y, Ye J, Han D, Cao X, Ding X, Zhang Y, Xu W, Orr J, Jen R, Sands S, Malhotra A, Owens R (2017) Physiology-based modeling may predict surgical treatment outcome for obstructive sleep apnea. J Clin Sleep Med 13:1029–1037. https://doi.org/10.5664/jcsm.6716